

Rényi formulation of uncertainty relations for POVMs assigned to a quantum design

Alexey E. Rastegin*

Department of Theoretical Physics, Irkutsk State University, Irkutsk 664003, Russia

Information entropies provide powerful and flexible way to express restrictions imposed by the uncertainty principle. This approach seems to be very suitable in application to problems of quantum information theory. It is typical that questions of such a kind involve measurements having one or another specific structure. The latter often allows us to improve entropic bounds that follow from uncertainty relations of sufficiently general scope. Quantum designs have found use in many issues of quantum information theory, whence uncertainty relations for related measurements are of interest. In this paper, we obtain uncertainty relations in terms of min-entropies and Rényi entropies for POVMs assigned to a quantum design. Relations of the Landau–Pollak type are addressed as well. Using examples of quantum designs in two dimensions, the obtained lower bounds are then compared with the previous ones. An impact on entropic steering inequalities is briefly discussed.

Keywords: uncertainty principle, quantum design, min-entropy, Rényi entropy

I. INTRODUCTION

The Heisenberg uncertainty principle [1] is widely recognized as a fundamental scientific concept. Since the first formal derivations of Kennard [2] and Robertson [3] appeared, many approaches and scenarios were addressed [4, 5]. In effect, the Heisenberg thought experiment with microscope should be treated as dealing with successive measurements. The scenario with successive measurements [6, 7] differs from the preparation one, when repeated trials with the same quantum state are dealt with [8]. An important question is how to characterize properly the amount of uncertainties in quantum measurements. The usual way in terms of lower bound on the product of variances has been criticized for several reasons [9, 10]. As an alternative, uncertainty bounds on the sum of variances were examined [11, 12]. Entropic uncertainty relations are currently the subject of active researches [13–17]. This approach allows us to strengthen uncertainty relations due to quantum side information [18–20] and connect them to fundamental properties of relative entropies [21]. Majorization technique is one of powerful tools to formulate the uncertainty principle [22–26]. Another way to find good entropic bounds is based on a direct optimization [27, 28]. Uncertainty relations for successive measurements have also been studied within the entropic approach [29–32].

Protocols of quantum information processing often deal with measurements having some special inner structure. Mutually unbiased bases are an especially important example reviewed, e.g., in the paper [33]. Symmetric informationally complete measurements (SIC-POVMs) give another helpful tool for manipulating quantum carriers of information. As the authors of [34] showed, the SIC-POVM problem is closely related to the concept of t -designs. The existence of SIC-POVMs can be studied both analytically and numerically, so that the list of solutions is permanently growing [35, 36]. The claim that SICs exist in every finite dimension is known as Zauner’s conjecture in its weakest form [37]. It is linked to a lot of purely mathematical questions, some of them are discussed in [38–41]. Initially, spherical t -designs on the unit sphere with some applications were studied in [42]. Quantum t -designs also known as complex projective designs have been examined for several reasons [43, 44]. In general, t -designs in projective spaces were considered in [45]. The concept of designs is shown to be useful for a wide range of information-theoretic applications [46–51].

Due to an interesting structure of quantum designs and their possible role in emerging technologies, we have come across several questions. In particular, one aims to characterize the amount of uncertainty in related quantum measurements. In comparison with the known general formulations, more accurate estimates can be given for quantum designs. Recently, the authors of [52] addressed entropic uncertainty relations for POVMs assigned to a quantum design. The used method is based on the monotonicity of certain vector norms. It also allows one to write uncertainty relations in terms of min-entropies. In general, these relations are not optimal. As was discussed in [53], for measurements with a special structure we can enhance an estimation of the corresponding min-entropies. For MUBs and SIC-POVMs, this improvement holds due to estimating indices of coincidence. It turns out that a similar approach can be developed for quantum designs. Although formulation becomes more complicated, the key idea is very similar to what was exploited in [53]. In effect, additional details are not difficult from the viewpoint of calculations.

*Electronic address: alexrastegin@mail.ru

The aim of this work is to study Rényi formulation of uncertainty relations for POVMs assigned to a quantum design. The proposed method mainly concentrates on a good estimation of min-entropies. It is a natural development of the idea considered in [53]. Due to a non-obvious application of Jensen's inequality, one can estimate the maximal probability from above. This estimate also allows us to improve entropic uncertainty relations for other values of the entropic parameter. The paper is organized as follows. The preliminary material on quantum designs is reviewed in Section II. In particular, we summarize some results on quantum designs and recall the used entropic functions. Section III is devoted to formulation of main results of the paper. In Section IV, we consider examples of application to concrete quantum designs as well as the comparison with the previously given entropic bounds. An application to entropic steering inequalities is briefly discussed. In Section V, we conclude the paper with a summary of the results.

II. DEFINITIONS AND NOTATION

In this section, we review the required material concerning quantum designs and used entropies. Several equivalent ways to define quantum designs were discussed in the literature. This concept can be treated as an extension of the analog structure on spheres in \mathbb{R}^d . A spherical t -design is a finite set of normalized real vectors such that the average value of any t th order polynomial over this set is equal to the average over all normalized vectors in \mathbb{R}^d . The original motivation for studying these objects came from the numerical evaluation of multi-dimensional integrals [54].

In the finite-dimensional Hilbert space \mathbb{C}^d , one considers lines passing through the origin, which form the complex projective space $\mathbb{C}P^{d-1}$ [43]. Up to a phase, each line can be represented by a unit vector $|\phi\rangle$ in \mathbb{C}^d . For a general discussion of complex projective spaces and related topics, see chapter 4 of [55]. The set $\mathbb{D} = \{|\phi_k\rangle : |\phi_k\rangle \in \mathbb{C}^d, \langle\phi_k|\phi_k\rangle = 1, k = 1, \dots, K\}$ is a complex projective t -design, when the following property holds [43]. For every real polynomial \mathcal{P}_t of degree at most t , the average value over \mathbb{D} is equal to the average value over all normalized vectors of \mathbb{C}^d , viz.

$$\frac{1}{K^2} \sum_{j,k=1}^K \mathcal{P}_t\left(|\langle\phi_j|\phi_k\rangle|^2\right) = \int \int d\mu(\psi) d\mu(\psi') \mathcal{P}_t\left(|\langle\psi|\psi'\rangle|^2\right). \quad (1)$$

By $\mu(\psi)$, one denotes here the unique unitarily-invariant probability measure on $\mathbb{C}P^{d-1}$ induced by the Haar measure on the corresponding unitary group. It is seen from the above definition that each t -design is also a s -design with $s \leq t$. It follows from the results of [56] that t -designs in $\mathbb{C}P^{d-1}$ exist for all t and d . Examples with smallest number of vectors are certainly difficult to construct. Even if the smallest number of points is not required, there is no general strategy to generate designs in all respective cases. In more detail, these questions are discussed in [57, 58]. In effect, there exist important examples that are widely used in applications. The concept of quantum designs is naturally connected to the problem of building SIC-POVMs and tight rank-one informationally complete POVMs [34, 43].

Complex projective designs have a lot of interesting properties. For a t -design, one has [43]

$$\frac{1}{K} \sum_{k=1}^K |\phi_k\rangle\langle\phi_k|^{\otimes t} = \mathcal{D}_d^{(t)} \Pi_{\text{sym}}^{(t)}, \quad (2)$$

where $\Pi_{\text{sym}}^{(t)}$ is the projector onto the symmetric subspace of $(\mathbb{C}^d)^{\otimes t}$. The number $\mathcal{D}_d^{(t)}$ is the inverse of dimensionality of the symmetric subspace, namely

$$\mathcal{D}_d^{(t)} = \binom{d+t-1}{t}^{-1} = \frac{t!(d-1)!}{(d+t-1)!}. \quad (3)$$

The role of projector $\Pi_{\text{sym}}^{(t)}$ was often emphasized in the literature. In principle, the formula (2) can be used as equivalent definition of a quantum t -design [43]. For the given t , this formula can be applied for all positive integers $s \leq t$. In particular, substituting $t = 1$ results in

$$\frac{d}{K} \sum_{k=1}^K |\phi_k\rangle\langle\phi_k| = \mathbb{1}_d. \quad (4)$$

Thus, unit vectors $|\phi_k\rangle$ lead to a resolution of the identity in \mathbb{C}^d . In principle, there may be several ways to assign a set of POVMs to the given t -design. These ways are unknown *a priori*, without an explicit consideration of kets $|\phi_k\rangle$. The only obvious case is to take the complete set \mathcal{E} consisting of operators

$$\mathbf{E}_k = \frac{d}{K} |\phi_k\rangle\langle\phi_k|. \quad (5)$$

We shall also address the case, when M rank-one POVMs $\{\mathcal{E}^{(m)}\}_{m=1}^M$ can be assigned to the given quantum design. Each of these POVMs consist of n operators of the form

$$\mathbf{E}_j^{(m)} = \frac{d}{n} |\phi_j^{(m)}\rangle\langle\phi_j^{(m)}|. \quad (6)$$

Here, the numbers n and M are connected by $K = nM$. In the following, we will discuss an example of quantum design, in which the kets form a set of mutually unbiased bases. When ways to choose a set of POVMs are determined, for each of them our method will give entropic uncertainty relations.

Let classical random variable Z take values according to discrete probability distribution $\{p(z)\}$. For $0 < \alpha \neq 1$, the Rényi α -entropy is defined as [59]

$$R_\alpha(Z) := \frac{1}{1-\alpha} \ln\left(\sum_z p(z)^\alpha\right). \quad (7)$$

This entropy does not increase with growth of α . For a discussion of basic properties of (7), see section 2.7 of [55]. In the limit $\alpha \rightarrow 1$, the right-hand side of (7) reduces to the Shannon entropy. In general, information-theoretic functions of the Rényi type do not succeed all the properties of the standard functions. In more detail, these questions are discussed in [60–63]. In particular, some popular measures to quantify mutual information are not completely legitimate in the context of quantum cryptography [64]. Nevertheless, the use of parametrized entropic functions may often provide additional possibilities in analysis [10]. A utility of generalized entropies in application to combinatorial issues was shown in [65]. The limit $\alpha \rightarrow \infty$ gives the so-called min-entropy

$$R_\infty(Z) = -\ln(\max p(z)). \quad (8)$$

Uncertainty relations in terms of min-entropies with some application were discussed in [66, 67]. In the following, min-entropies will be used in posing uncertainty relations for quantum designs.

If the pre-measurement state is described by density matrix ρ of unit trace, then the probability of j th outcome is equal to

$$p_j(\mathcal{E}^{(m)}; \rho) = \frac{d}{n} \langle\phi_j^{(m)}|\rho|\phi_j^{(m)}\rangle. \quad (9)$$

Substituting (9) into (7) leads to the entropy $R_\alpha(\mathcal{E}^{(m)}; \rho)$. It follows from (2) that, for any density matrix ρ and the given t -design, one has [52]

$$\frac{1}{K} \sum_{k=1}^K \langle\phi_k|\rho|\phi_k\rangle^t = \mathcal{D}_d^{(t)} \text{tr}(\rho^{\otimes t} \Pi_{\text{sym}}^{(t)}). \quad (10)$$

Combining (9) with (10) then gives

$$\sum_{m=1}^M \sum_{j=1}^n p_j(\mathcal{E}^{(m)}; \rho)^t = \left(\frac{d}{n}\right)^t \sum_{k=1}^K \langle\phi_k|\rho|\phi_k\rangle^t = K n^{-t} d^t \mathcal{D}_d^{(t)} \text{tr}(\rho^{\otimes t} \Pi_{\text{sym}}^{(t)}). \quad (11)$$

When a single POVM is assigned, we have $n = K$ and

$$\sum_{k=1}^K p_k(\mathcal{E}; \rho)^t = K^{1-t} d^t \mathcal{D}_d^{(t)} \text{tr}(\rho^{\otimes t} \Pi_{\text{sym}}^{(t)}). \quad (12)$$

The formulas (11) and (12) also holds with $s = 2, \dots, t$ instead of t . The authors of [52, 68] described how to express $\text{tr}(\rho^{\otimes t} \Pi_{\text{sym}}^{(t)})$ as a sum of monomials of the moments $\text{tr}(\rho^q)$. In particular, it holds that

$$\text{tr}(\rho^{\otimes 2} \Pi_{\text{sym}}^{(2)}) = \frac{1}{2} [1 + \text{tr}(\rho^2)], \quad (13)$$

$$\text{tr}(\rho^{\otimes 3} \Pi_{\text{sym}}^{(3)}) = \frac{1}{6} [1 + 3 \text{tr}(\rho^2) + 2 \text{tr}(\rho^3)], \quad (14)$$

$$\text{tr}(\rho^{\otimes 4} \Pi_{\text{sym}}^{(4)}) = \frac{1}{24} [1 + 6 \text{tr}(\rho^2) + 3 \text{tr}(\rho^2)^2 + 8 \text{tr}(\rho^3) + 6 \text{tr}(\rho^4)]. \quad (15)$$

With growth of t , expressions of this kind become more complicated. It is useful to note that

$$d^t \mathcal{D}_d^{(t)} \operatorname{tr}(\rho_*^{\otimes t} \Pi_{\text{sym}}^{(t)}) = 1 \leq d^t \mathcal{D}_d^{(t)} \operatorname{tr}(\rho^{\otimes t} \Pi_{\text{sym}}^{(t)}), \quad (16)$$

where $\rho_* = d^{-1} \mathbb{1}_d$ is the maximally mixed state. Combining (12) with (16) and $\operatorname{tr}(\rho^{\otimes t} \Pi_{\text{sym}}) \leq 1$ finally gives

$$K^{1-t} \leq \sum_{k=1}^K p_k(\mathcal{E}; \rho)^t \leq K^{1-t} d^t \mathcal{D}_d^{(t)}. \quad (17)$$

The right inequality will be used to obtain state-independent uncertainty relations. In the following, we will deal with examples, where the right-hand side of (17) is sufficiently small in comparison with 1.

Finally, the main results of the paper [52] will be recalled. To avoid bulky expressions, we introduce the two parameters

$$\bar{\beta}_n = n^{1-t} d^t \mathcal{D}_d^{(t)} \operatorname{tr}(\rho^{\otimes t} \Pi_{\text{sym}}^{(t)}), \quad (18)$$

$$\bar{\beta} = K^{1-t} d^t \mathcal{D}_d^{(t)} \operatorname{tr}(\rho^{\otimes t} \Pi_{\text{sym}}^{(t)}). \quad (19)$$

The latter follows from (18) by substituting $n = K$. Let M rank-one POVMs $\mathcal{E}^{(m)}$ be assigned to the given t -design. For $\alpha \geq t$, the average α -entropy satisfies [52]

$$\frac{1}{M} \sum_{m=1}^M R_\alpha(\mathcal{E}^{(m)}; \rho) \geq \frac{\alpha}{t(1-\alpha)} \ln \bar{\beta}_n. \quad (20)$$

For the case of a single POVM, the above uncertainty relation reduces to

$$R_\alpha(\mathcal{E}; \rho) \geq \frac{\alpha}{t(1-\alpha)} \ln \bar{\beta}, \quad (21)$$

These results are derived from (11) and (12) due to monotonicity of the vector p -norm and the function $y \mapsto -\ln y$. The inequalities (20) and (21) remain valid for s instead of t and $\alpha \geq s$, provided that integer s lies between 2 and t . According to (20) and (21), the min-entropies obey

$$\frac{1}{M} \sum_{m=1}^M R_\infty(\mathcal{E}^{(m)}; \rho) \geq -\frac{1}{t} \ln \bar{\beta}_n, \quad (22)$$

$$R_\infty(\mathcal{E}; \rho) \geq -\frac{1}{t} \ln \bar{\beta}. \quad (23)$$

As will be shown, the uncertainty relations (20)–(23) can be improved. The authors of [52] also formulated uncertainty relations in terms of Tsallis entropies. Such entropies are not considered in the following.

III. MAIN RESULTS

This section is devoted to deriving Rényi-entropy uncertainty relations for POVMs assigned to a quantum design. We begin with a discussion of min-entropy uncertainty relations. To obtain uncertainty relations from (11) and (12), we will use an auxiliary consideration. Let n positive numbers y_j obey the two relations

$$\sum_{j=1}^n y_j = 1, \quad (24)$$

$$\sum_{j=1}^n y_j^t = \beta. \quad (25)$$

It follows from the normalization (24) that $n^{1-t} \leq \beta \leq 1$. We aim to estimate maximum of the numbers y_j from above. For definiteness, we assume that these numbers are arranged in non-decreasing order, so that $y_j \leq y_n$. By convexity of the function $y \mapsto y^t$ for $t > 1$, one has

$$\left(\frac{1}{n-1} \sum_{j=1}^{n-1} y_j \right)^t \leq \frac{1}{n-1} \sum_{j=1}^{n-1} y_j^t. \quad (26)$$

Combining the left- and right-hand sides of (26) respectively with (24) and with (25) finally gives

$$\frac{(1-y_n)^t}{(n-1)^{t-1}} \leq \beta - y_n^t. \quad (27)$$

To estimate y_n from above, one should solve

$$\frac{(1-y)^t}{(n-1)^{t-1}\beta} + \frac{y^t}{\beta} = 1. \quad (28)$$

Restricting a consideration to the quadrant I , we wish to find coordinates of the intersection of the curve

$$\frac{x^t}{(n-1)^{t-1}\beta} + \frac{y^t}{\beta} = 1 \quad (29)$$

with the straightforward line $x+y=1$. The curve intersects the axes with the abscissa $(n-1)^{1-1/t}\beta^{1/t}$ and with the ordinate $\beta^{1/t}$. For even t , the equation (29) gives an oval line symmetric with respect to both the axes. It bounds the convex set on the plane. The points of this oval line lie between the ellipse with the above semi-axes and the corresponding rectangle, closely to the latter. Here, we have two intersection points or one point of touching the line $x+y=1$. With growth of even t , the curve (29) will mimic a rectangle with rounded corners. For odd t , the curve goes inside the mentioned rectangle only in the quadrant I . Beyond this quadrant, the curve tends to go along the asymptote

$$y = -\frac{x}{(n-1)^{1-1/t}}. \quad (30)$$

When $n > 2$, the latter intersects $x+y=1$ in the quadrant IV . Hence, we conclude that there is two or three intersection points. In all the cases, we are interested in the point with maximal ordinate.

By $\Upsilon_{n-1}^{(t)}(\beta)$, we further denote the maximal real root of (28). Some properties of $\Upsilon_{n-1}^{(t)}(\beta)$ as a function of β are discussed in Appendix A. Let us mention a special case to be discussed explicitly. For $\beta = n^{1-t}$, the equation (28) has the root $y_n = 1/n$, so that

$$\Upsilon_{n-1}^{(t)}(n^{1-t}) = \frac{1}{n}. \quad (31)$$

Writing the latter as $\beta^{1/(t-1)}$ with $t \geq 2$, one can expect concavity and increasing, at least in some neighborhood. The answer (31) is naturally explained as follows. For the maximally mixed state, we have $p_j(\mathcal{E}^{(m)}; \rho_*) = 1/n$ irrespectively to j . Hence, the maximal probability is given by (31). For $n = K$, the left-hand side of (17) is also reached with the maximally mixed state.

For $t \geq 5$, one is generally unable to express $\Upsilon_{n-1}^{(t)}(\beta)$ analytically using radicals. On the other hand, for the given parameters the answer can always be found by appropriate numerical procedure with any desired accuracy. In the cases $t = 2, 3, 4$, we can express the answer in a closed analytic form. The case $t = 2$ is the simplest one, when

$$\Upsilon_{n-1}^{(2)}(\beta) = \frac{1}{n} \left(1 + \sqrt{n-1} \sqrt{n\beta-1} \right). \quad (32)$$

This result was derived and applied to uncertainty relations in the paper [53]. Some useful formulas for $t = 3$ are given in Appendix B. Due to the above consideration, the following statement takes place.

Proposition 1 *Let M rank-one POVMs $\mathcal{E}^{(m)}$, each with n elements of the form (6), be assigned to a quantum t -design $\mathbb{D} = \{|\phi_k\rangle\}_{k=1}^K$ in d dimensions. If the pre-measurement state is described by the density matrix ρ , then*

$$\frac{1}{M} \sum_{m=1}^M R_\infty(\mathcal{E}^{(m)}; \rho) \geq -\ln(\Upsilon_{n-1}^{(t)}(\bar{\beta}_n)), \quad (33)$$

where $\Upsilon_{n-1}^{(t)}(\beta)$ denotes the maximal real root of (28) and $\bar{\beta}_n$ is defined by (18).

Proof. It follows from the preliminary consideration that, for all $m = 1, \dots, M$,

$$\max_j p_j(\mathcal{E}^{(m)}; \rho) \leq \Upsilon_{n-1}^{(t)}(\beta_m), \quad (34)$$

where

$$\beta_m = \sum_{j=1}^n p_j(\mathcal{E}^{(m)}; \boldsymbol{\rho})^t.$$

Combining (8) with (34) then gives $R_\infty(\mathcal{E}^{(m)}; \boldsymbol{\rho}) \geq -\ln(\Upsilon_{n-1}^{(t)}(\beta_m))$, whence we write

$$\frac{1}{M} \sum_{m=1}^M R_\infty(\mathcal{E}^{(m)}; \boldsymbol{\rho}) \geq \sum_{m=1}^M \frac{1}{M} [-\ln(\Upsilon_{n-1}^{(t)}(\beta_m))] \geq -\ln\left(\sum_{m=1}^M \frac{1}{M} \Upsilon_{n-1}^{(t)}(\beta_m)\right) \quad (35)$$

$$\geq -\ln \Upsilon_{n-1}^{(t)}\left(\sum_{m=1}^M \frac{\beta_m}{M}\right). \quad (36)$$

The steps (35) and (36) respectively hold due to convexity and decreasing of the function $y \mapsto -\ln y$, with adding

$$\sum_{m=1}^M \frac{1}{M} \Upsilon_{n-1}^{(t)}(\beta_m) \leq \Upsilon_{n-1}^{(t)}\left(\sum_{m=1}^M \frac{\beta_m}{M}\right).$$

The latter is valid due to concavity of $\Upsilon_{n-1}^{(t)}(\beta)$ with respect to β (this fact is shown in Appendix A). Combining (36) with (11) and $K = nM$ completes the proof of (33). ■

When single POVM \mathcal{E} with K elements (5) is assigned to the given t -design, the inequality (33) reduces to

$$R_\infty(\mathcal{E}; \boldsymbol{\rho}) \geq -\ln(\Upsilon_{K-1}^{(t)}(\bar{\beta})), \quad (37)$$

where $\bar{\beta}$ is defined by (19). The results (33) and (37) provide state-dependent uncertainty relations in terms of min-entropies. In particular, the second one is expressed in terms of the single parameter (19). The result (37) cannot further be improved without using additional data about the actual pre-measurement state. As the function $y \mapsto -\ln y$ decreases, we also have

$$\frac{1}{M} \sum_{m=1}^M R_\infty(\mathcal{E}^{(m)}; \boldsymbol{\rho}) \geq -\ln(\Upsilon_{n-1}^{(t)}(n^{1-t} d^t \mathcal{D}_d^{(t)})), \quad (38)$$

$$R_\infty(\mathcal{E}; \boldsymbol{\rho}) \geq -\ln(\Upsilon_{K-1}^{(t)}(K^{1-t} d^t \mathcal{D}_d^{(t)})). \quad (39)$$

These state-independent formulations hold for all states and correspond to substituting the right-hand side of (17).

The presented method immediately leads to uncertainty relations of the Landau–Pollak type. The original results of Landau and Pollak concern uncertainty in signal theory [69]. The authors of [10] gave reformulation to characterize the amount of uncertainty in projective quantum measurements. Extensions to POVM measurements were formulated in [70, 71]. In contrast to projective measurements, for a single rank-one POVM we may have a non-trivial upper bound on the maximal probability. This takes place, when number of outcomes exceeds the dimensionality. Due to (34) and concavity of $\Upsilon_{n-1}^{(t)}(\beta)$ with respect to β , we obtain

$$\frac{1}{M} \sum_{m=1}^M \max_j p_j(\mathcal{E}^{(m)}; \boldsymbol{\rho}) \leq \sum_{m=1}^M \frac{1}{M} \Upsilon_{n-1}^{(t)}(\beta_m) \leq \Upsilon_{n-1}^{(t)}(\bar{\beta}_n), \quad (40)$$

$$\max_k p_k(\mathcal{E}; \boldsymbol{\rho}) \leq \Upsilon_{K-1}^{(t)}(\bar{\beta}), \quad (41)$$

These relations can be used in formulating criteria to characterize entanglement or steerability. For instance, the writers of [72] considered separability conditions based on the Landau–Pollak uncertainty relation.

The Newton–Raphson method is a well-known numerical algorithm for finding roots of equations. In application to $f(y) = 0$ with some initial guess $y^{(0)}$, this method gives a correction

$$y^{(1)} - y^{(0)} = -\frac{f(y^{(0)})}{f'(y^{(0)})}. \quad (42)$$

The value $y^{(1)}$ is a better approximation of the root than $y^{(0)}$. By repeating such steps, one is able to improve approximations successively. In order to calculate $\Upsilon_{n-1}^{(t)}(\bar{\beta}_n)$, we can start the process with the value $\bar{\beta}_n^{1/t}$. The latter is larger than the desired root, since the condition (25) for $\beta = \bar{\beta}_n$ implies

$$y_j^t \leq \bar{\beta}_n.$$

In the case of interest, we use the function $y \mapsto (n-1)^{t-1}y^t + (1-y)^t - (n-1)^{t-1}\bar{\beta}_n$. The latter is obviously convex and increasing for $y > 1/n$. Substituting $\bar{\beta}_n^{1/t}$ then implies a positive value of the function, which should vanish for the desired point. Since the Newton–Raphson method replaces the function with its tangent line, the first step will result in the term that exceeds the root due to convexity. In other words, we have

$$\Upsilon_{n-1}^{(t)}(\bar{\beta}_n) \leq \tilde{\Upsilon}_{n-1}^{(t)}(\bar{\beta}_n) = \bar{\beta}_n^{1/t} - \frac{(1 - \bar{\beta}_n^{1/t})^t}{t(n-1)^{t-1}\bar{\beta}_n^{1-1/t} - t(1 - \bar{\beta}_n^{1/t})^{t-1}}. \quad (43)$$

This explicit expression is slightly complicated, but quite suitable to calculate. Combining (33) and (37) with (43), one gets

$$\frac{1}{M} \sum_{m=1}^M R_\infty(\mathcal{E}^{(m)}; \boldsymbol{\rho}) \geq -\ln(\tilde{\Upsilon}_{n-1}^{(t)}(\bar{\beta}_n)), \quad (44)$$

$$R_\infty(\mathcal{E}; \boldsymbol{\rho}) \geq -\ln(\tilde{\Upsilon}_{K-1}^{(t)}(\bar{\beta})). \quad (45)$$

That is, one Newton–Raphson step gives valid inequalities whose right-hand sides can be expressed analytically. Due to positivity and convexity, repeated steps of such a kind will further improve our result. However, the corresponding expressions are sufficiently bulky.

Due to (33), we can also estimate the average α -entropy from below for all $\alpha \geq t$. This is obtained by some extension of the reasons proposed in [73]. For $\alpha \geq t$, we merely write

$$\sum_z p(z)^\alpha \leq (\max_z p(z))^{\alpha-t} \sum_z p(z)^t. \quad (46)$$

The latter together with (7) implies

$$R_\alpha(Z) \geq \frac{\alpha-t}{\alpha-1} R_\infty(Z) + \frac{t-1}{\alpha-1} R_t(Z), \quad (47)$$

whenever $\alpha \geq t \geq 1$. It follows from (20) that

$$\frac{1}{M} \sum_{m=1}^M R_t(\mathcal{E}^{(m)}; \boldsymbol{\rho}) \geq -\frac{\ln \bar{\beta}_n}{t-1}. \quad (48)$$

Combining (33), (47) and (48), we have arrived at a conclusion.

Proposition 2 *Let M rank-one POVMs $\mathcal{E}^{(m)}$, each with n elements of the form (6), be assigned to a quantum t -design $\mathbb{D} = \{|\phi_k\rangle\}_{k=1}^K$ in d dimensions. For $\alpha \geq t$, it holds that*

$$\frac{1}{M} \sum_{m=1}^M R_\alpha(\mathcal{E}^{(m)}; \boldsymbol{\rho}) \geq -\frac{\alpha-t}{\alpha-1} \ln(\Upsilon_{n-1}^{(t)}(\bar{\beta}_n)) - \frac{\ln \bar{\beta}_n}{\alpha-1}, \quad (49)$$

where $\Upsilon_{n-1}^{(t)}(\beta)$ denotes the maximal real root of (28) and $\bar{\beta}_n$ is defined by (18).

When single POVM \mathcal{E} with K elements (5) is assigned to the given t -design, the inequality (49) reduces to

$$R_\alpha(\mathcal{E}; \boldsymbol{\rho}) \geq -\frac{\alpha-t}{\alpha-1} \ln(\Upsilon_{K-1}^{(t)}(\bar{\beta})) - \frac{\ln \bar{\beta}}{\alpha-1}, \quad (50)$$

where $\bar{\beta}$ is defined by (19). Substituting $\bar{\beta}_n = n^{1-t}d^t \mathcal{D}_d^{(t)}$ into (49) leads to the state-independent formulation

$$\frac{1}{M} \sum_{m=1}^M R_\alpha(\mathcal{E}^{(m)}; \boldsymbol{\rho}) \geq -\frac{\alpha-t}{\alpha-1} \ln(\Upsilon_{n-1}^{(t)}(n^{1-t}d^t \mathcal{D}_d^{(t)})) - \frac{\ln(n^{1-t}d^t \mathcal{D}_d^{(t)})}{\alpha-1}. \quad (51)$$

Let us compare new entropic bounds with the previous ones. For brevity, we focus on the results (21) and (50). It is instructive to apply them to the maximally mixed state $\boldsymbol{\rho}_*$. Using $\bar{\beta} = K^{1-t}$ and (31), one gets

$$R_\alpha(\mathcal{E}; \boldsymbol{\rho}_*) \geq \frac{\alpha-t}{\alpha-1} \ln K + \frac{t-1}{\alpha-1} \ln K = \ln K. \quad (52)$$

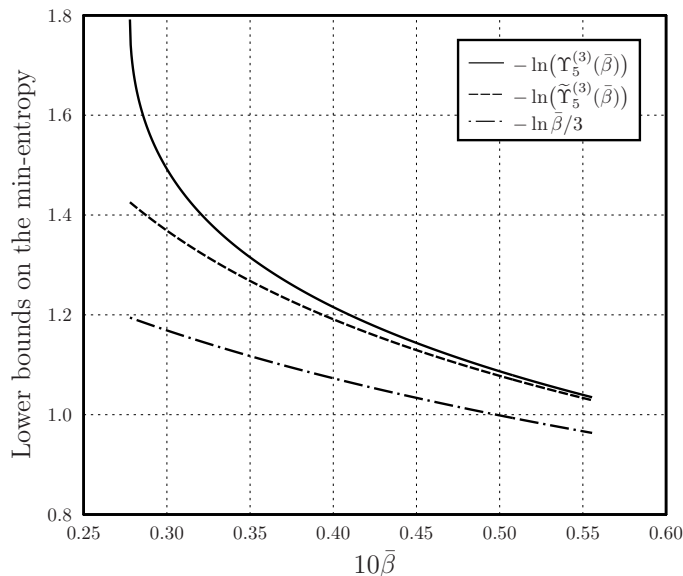


FIG. 1: The three lower bounds on the min-entropy versus the parameter (19) for the 3-design. For convenience of presentation, the abscissa shows $10\bar{\beta}$.

In other words, the uncertainty relation (50) is saturated with the maximally mixed state. At the same time, the relation (21) reads here as

$$R_\alpha(\mathcal{E}; \rho_*) \geq \frac{\alpha(t-1)}{t(\alpha-1)} \ln K. \quad (53)$$

Restricting to $\alpha \geq t$, the latter coincides with (52) only for $\alpha = t$. For sufficiently large α , the difference between these bounds is approximately $\ln K/t$. Thus, the result (50) sometimes provides a considerable improvement of (21). Taking $\alpha = \infty$, the ratio of the right-hand sides of (52) and (53) is $t/(t-1)$. The latter implies 1.5 for 3-designs and 1.25 for 5-designs. For other states, when $\bar{\beta} > K^{1-t}$, the amount of improvement is lesser. Nevertheless, the inequality (50) is stronger than (21). In a similar manner, the result (49) somehow enhances (20).

IV. EXAMPLES OF UNCERTAINTY BOUNDS FOR QUANTUM DESIGNS

In this section, we consider examples of application of the developed method to concrete quantum designs in two dimensions. The short description of these designs in terms of components of the Bloch vector can be found in [52]. The corresponding vertices form some polyhedron. We will mainly focus on the case of single assigned POVM. It is instructive to visualize distinctions between the lower estimates (23), (37), and (45). Note that the right-hand side of (45) can be treated as an improvement of (23) within the first Newton–Raphson step. In general, the significance of correction depends on the quantity (19).

Let us begin with the 3-design with $K = 6$ vertices forming an octahedron. The quantity $\Upsilon_5^{(3)}(\bar{\beta})$ is calculated in line with the formulas listed in Appendix B. In Fig. 1, we plot the lower bounds (23), (37), and (45). In general, the improvement due to both the formulas (37) and (45) is considerable. The right-hand sides of (37) and (45) are close for pure states and states with a low mixedness. Here, these results enhance the right-hand side of (23) by values of order 7 %. For small values of $\bar{\beta}$, when the measured state is close to the maximally mixed one, we see essential distinctions between all the three uncertainty bounds. Due to (37), we improve the lower entropic bound in comparison with (23) approximately 1.5 times. Overall, the results (37) and (45) provide a good improvement.

The example with octahedron is interesting in additional respect due to the following. The considered 3-design is formed by eigenstates of the Pauli matrices. That is, the complete set of three mutually unbiased bases are assigned to this 3-design. Entropic uncertainty relations for such bases have attracted a lot of attention. The three bases associated with Pauli’s matrices are traditionally used as a test. Restricting a consideration to min-entropies, we shall

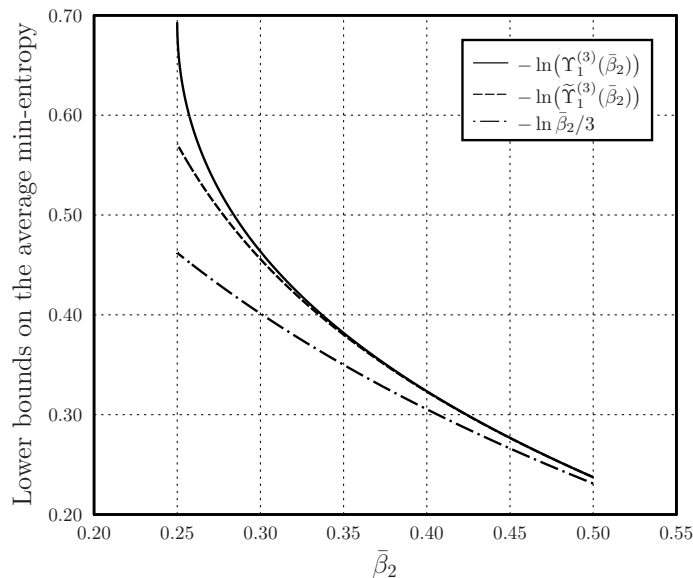


FIG. 2: The three lower bounds on the average min-entropy for the three mutually unbiased bases in two dimensions.

discuss them in more detail. Substituting $M = 3$ and $n = 2$, the formula (33) reads as

$$\frac{1}{3} \sum_{m=1}^3 R_{\infty}(\mathcal{E}^{(m)}; \rho) \geq -\ln(\Upsilon_1^{(3)}(\bar{\beta}_2)) = -\ln\left(\frac{\sqrt{3} + (4\bar{\beta}_2 - 1)^{1/2}}{2\sqrt{3}}\right), \quad (54)$$

where we used (B4). One has $\bar{\beta}_2 = [1 + 3 \text{tr}(\rho^2) + 2 \text{tr}(\rho^3)]/12$ due to (14) and (18). The relation (54) should be compared with the inequality

$$\frac{1}{3} \sum_{m=1}^3 R_{\infty}(\mathcal{E}^{(m)}; \rho) \geq -\frac{\ln \bar{\beta}_2}{3}, \quad (55)$$

which follows from (22). Another uncertainty relation in terms of the purity $\text{tr}(\rho^2)$ was proved in [53]. For $M = 3$ and $d = 2$, it reads as

$$\frac{1}{3} \sum_{m=1}^3 R_{\infty}(\mathcal{E}^{(m)}; \rho) \geq \ln\left(\frac{2\sqrt{3}}{\sqrt{3} + \sqrt{2 \text{tr}(\rho^2) - 1}}\right). \quad (56)$$

Dealing with two dimensions, we have $\bar{\beta}_2 = 0.5 - \lambda + \lambda^2$ and $\text{tr}(\rho^2) = 1 - 2\lambda + 2\lambda^2 = 2\bar{\beta}_2$, where λ is the minimal eigenvalue of ρ . Hence, the right-hand side of (54) is equal to the right-hand side of (56). In other words, the result (54) reproduces the previous one from [53]. Note that both the inequalities (54) and (56) are based on an estimation of the maximal probability from above. To compare these inequalities with (55), we plot the lower bounds on the average min-entropy in Fig. 2. For a unification with other pictures, the curve $\bar{\beta}_2 \mapsto -\ln(\tilde{\Upsilon}_1^{(3)}(\bar{\beta}_2))$ is shown as well. In effect, the picture is generally similar to what is seen in Fig. 1. Distinctions between estimates are maximal on the left point, when $\bar{\beta}_2$ takes its minimal acceptable value. For very mixed states, the inequalities (54) and (56) exceed the right-hand side of (55) almost 1.5 times. For pure states, our curves improve the right-hand side of (55) by values of order 3 %.

The following example is the 5-design with $K = 12$ vertices forming an icosahedron. The quantity $\Upsilon_{11}^{(5)}(\bar{\beta})$ was calculated by means of the Newton–Raphson method. In Fig. 3, we plot the bounds (23), (37), and (45) for this example. Like the example with octahedron, the improvement due to both the formulas (37) and (45) turns out to be significant. In effect, the difference between (37) and (45) is maximal for sufficiently mixed states. For pure states, these results enhance the right-hand side of (23) by values of order 1 %. For small values of $\bar{\beta}$, the right-hand side of (37) exceeds the lower entropic bound (23) approximately 1.25 times. In general, reached improvements are considerable. Even in the state-independent formulation, they are of interest.

There is also the 5-design with $K = 30$ vertices forming an icosidodecahedron. On the average, actual values of probabilities becomes lesser in view of increased number of outcomes. In addition, acceptable values of the parameter

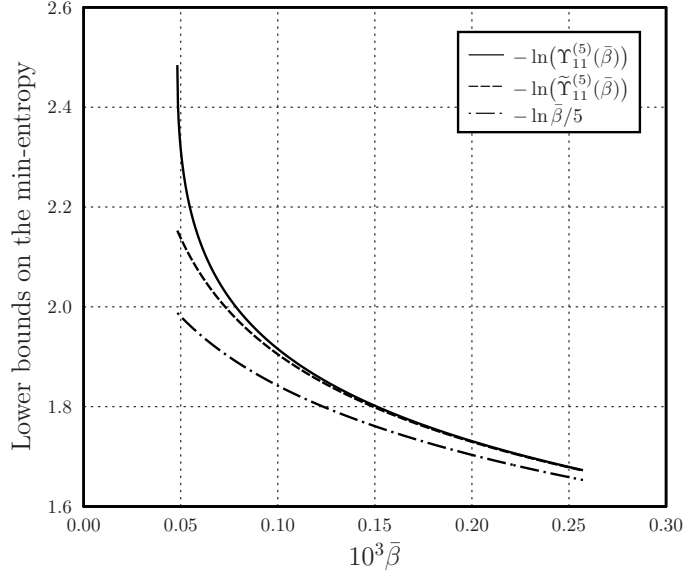


FIG. 3: The three lower bounds on the min-entropy versus the parameter (19) for the 5-design with 12 vertices. For convenience of presentation, the abscissa shows $10^3 \bar{\beta}$.

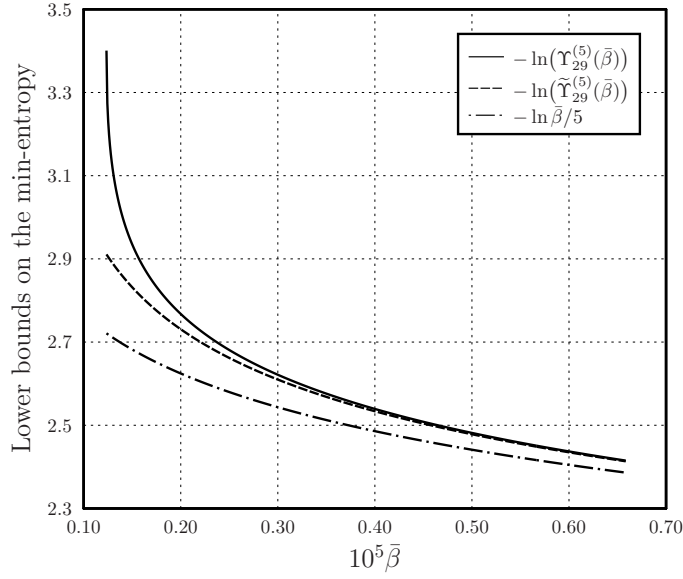


FIG. 4: The three lower bounds on the min-entropy versus the parameter (19) for the 5-design with 30 vertices. For convenience of presentation, the abscissa shows $10^5 \bar{\beta}$.

(19) are lesser than in the previous example. In Fig. 4, we plot the bounds (23), (37), and (45) for the example with icosidodekahedron. The general picture is quite similar to what is seen on Fig. 3. When $\bar{\beta}$ is close to its maximal acceptable value, the difference between (37) and (23) is relatively small, whereas the lower bounds (37) and (45) become coinciding. For small values of $\bar{\beta}$, distinctions between the three bounds are significant too. Overall, this example also characterizes a performance of the uncertainty relations (37) and (45).

We have compared the uncertainty relations (23), (37), and (45) within the three examples of quantum designs in two dimensions. It turned out that both the results (37) and (45) allow us to reach improved bounds. In the state-independent formulation, there is no essential distinctions between the results (37) and (45). When we know $\text{tr}(\rho^{\otimes t} \Pi_{\text{sym}}^{(t)})$ exactly or approximately, the uncertainty relation (37) is clearly preferable. The difference between the new bounds and (23) is minimal for pure states, when $\bar{\beta} = K^{1-t} d^t \mathcal{D}_d^{(t)}$. For $d = 2$, this difference is comparatively

small. It can be estimated due to the formulation (45). Indeed, we have

$$-\ln(\tilde{\Upsilon}_{K-1}^{(t)}(\bar{\beta})) + \frac{1}{t} \ln \bar{\beta} = -\ln(1 - \chi_{K-1}^{(t)}(\bar{\beta})) \geq \chi_{K-1}^{(t)}(\bar{\beta}), \quad (57)$$

$$\chi_{K-1}^{(t)}(\bar{\beta}) = \frac{\bar{\beta}^{-1/t} (1 - \bar{\beta}^{1/t})^t}{t(K-1)^{t-1} \bar{\beta}^{1-1/t} - t(1 - \bar{\beta}^{1/t})^{t-1}}.$$

Substituting $\bar{\beta} = K^{1-t} d^t \mathcal{D}_d^{(t)}$, we can estimate the mentioned difference. Overall, the quantity $\chi_{K-1}^{(t)}(\bar{\beta})$ *per se* provides sufficiently precise characterization. The result (57) gives a simple tool of comparing the two state-independent formulations for quantum designs with other values of d and K .

The derived uncertainty relations directly lead to entropic steering inequalities. The phenomenon of steering initially noticed by Schrödinger was rigorously formalized in [74]. For a general discussion of this important issue, see the review [75] and references therein. The writers of [76] focused on steering inequalities involving two entropies, but an extension to more items is straightforward [52]. The following conditions were formulated in [76]. First, the considered entropic uncertainty relations should be true, when they are conditioned on a classical random variable. The respective argument in application to Rényi entropies was presented in [76]. Second, the considered entropies should be non-increasing under conditioning on additional information. In view of the first restriction, we have to use the state-independent formulation of uncertainty relations.

To convert (49) into entropic steering inequality, a conditional form of the Rényi entropy should be incorporated. There is no generally accepted definition of conditional Rényi entropy [77, 78]. For a non-negative real order α , Arimoto [79] suggested the definition

$$R_\alpha(X|Z) := \frac{\alpha}{1-\alpha} \ln \left\{ \sum_z p(z) \left(\sum_x p(x|z)^\alpha \right)^{1/\alpha} \right\}. \quad (58)$$

The corresponding conditional min-entropy is written as [80]

$$R_\infty(X|Z) := -\ln \left(\sum_z p(z) \max_x p(x|z) \right). \quad (59)$$

Properties of these entropies with some applications are discussed in [78, 80]. In particular, the above conditional entropy cannot increase under conditioning on additional information. This property was originally proved by Arimoto [79] and reconsidered later in [78]. So, the entropies (58) and (59) obey the second condition formulated in [76].

Suppose that Alice and Bob share a bipartite quantum state ρ_{AB} , and repeat this any number of times. Alice performs on her subsystem a measurement chosen from the set of POVMs $\{\mathcal{F}^{(m)}\}_{m=1}^M$. So, the actual state of Bob's subsystem is conditioned on Alice's result. Bob's conditioned state is subjected to a measurement chosen accordingly from the set $\{\mathcal{E}^{(m)}\}_{m=1}^M$. We consider measurements assigned to a quantum t -design. Using the generated probabilities and classical side information from Alice, Bob takes the conditional α -entropies $R_\alpha(\mathcal{E}^{(m)}|\mathcal{F}^{(m)})$ according to (58). The latter depends on a shared state, though we do not mark this dependence explicitly. Following the approach of [52, 76], the inequality (51) leads to

$$\frac{1}{M} \sum_{m=1}^M R_\alpha(\mathcal{E}^{(m)}|\mathcal{F}^{(m)}) \geq -\frac{\alpha-t}{\alpha-1} \ln(\Upsilon_{n-1}^{(t)}(n^{1-t} d^t \mathcal{D}_d^{(t)})) - \frac{\ln(n^{1-t} d^t \mathcal{D}_d^{(t)})}{\alpha-1}, \quad (60)$$

where $\alpha \geq t$. The entropic steering inequality (60) allows us to enhance somehow the steering inequalities given in [52]. Due to the state-independent form of (40), we have another steering inequality

$$\frac{1}{M} \sum_{m=1}^M \sum_{\ell} p_{\ell}(\mathcal{F}^{(m)}; \rho_A) \max_j p_j(\mathcal{E}^{(m)}; \rho_{B\ell}^{(m)}) \leq \Upsilon_{n-1}^{(t)}(n^{1-t} d^t \mathcal{D}_d^{(t)}), \quad (61)$$

where the reduced densities are defined by $\rho_A = \text{tr}_B(\rho_{AB})$ and

$$p_{\ell}(\mathcal{F}^{(m)}; \rho_A) \rho_{B\ell}^{(m)} = \text{tr}_A \{ (\mathbb{F}_{\ell}^{(m)} \otimes \mathbb{1}_d)^{1/2} \rho_{AB} (\mathbb{F}_{\ell}^{(m)} \otimes \mathbb{1}_d)^{1/2} \}.$$

In principle, relations in terms of maximal probabilities may be more suitable in some questions. Applications of (40) and (41) to posing entanglement and steerability criteria could be the subject of separate research.

V. CONCLUSIONS

New uncertainty relations in terms of Rényi entropies were derived for POVM measurements assigned to a quantum design. The method used is a natural extension of the argument proposed in [53]. The principal point is to estimate from above the average maximal probability. It is possible due to the fact that the sum of powers t of rescaled probabilities is calculated exactly for a quantum t -design. The corresponding answer is expressed via trace of the projector onto the symmetric subspace of t -fold tensor-product space. Using done estimate of the average maximal probability, we immediately obtain uncertainty relations in terms of min-entropies as well as relations of the Landau–Pollak type. Moreover, one has easily obtained lower bounds on the average α -entropy for arbitrary $\alpha \geq t$.

The presented uncertainty relations are expressed in terms of specific root of algebraic equation of power t . Except for simple cases, this root cannot be expressed analytically using radicals. Nevertheless, the Newton–Raphson method is quite applicable in all particular situations. On the other hand, the first Newton–Raphson step leads to the explicit bound written analytically. Moreover, such an estimation is sufficiently good in the state-independent formulation. It must be stressed that for the maximally mixed state our lower bound on the min-entropy is saturated. A utility of the new bounds was demonstrated within several examples of quantum designs in two dimensions. Also, we briefly discussed steering inequalities based on the derived uncertainty relations.

Appendix A: Some properties of roots of the interest

This appendix aims to show that, for fixed t and n , the quantity $\Upsilon_{n-1}^{(t)}(\beta)$ is increasing and concave with respect to β . We restrict our consideration to the case $t \geq 2$ and $n \geq 2$. Let us consider the equation

$$(n-1)^{t-1}y^t + (1-y)^t = (n-1)^{t-1}\beta. \quad (\text{A1})$$

The quantity $\Upsilon_{n-1}^{(t)}(\beta)$ is defined as the maximal real root of this equation. Taking the derivative of both the sides of (A1) with respect to β gives

$$t \frac{\partial y}{\partial \beta} [(n-1)^{t-1}y^{t-1} - (1-y)^{t-1}] = (n-1)^{t-1}. \quad (\text{A2})$$

The equality $(n-1)^{t-1}y^{t-1} = (1-y)^{t-1}$ implies $y = 1/n$, whence $(n-1)^{t-1}y^{t-1} > (1-y)^{t-1}$ for $y > 1/n$. Combining this with (A2) results in the inequality $\partial y / \partial \beta > 0$. For the second derivative, we get

$$t \frac{\partial^2 y}{\partial \beta^2} [(n-1)^{t-1}y^{t-1} - (1-y)^{t-1}] + t(t-1) \left(\frac{\partial y}{\partial \beta} \right)^2 [(n-1)^{t-1}y^{t-2} + (1-y)^{t-2}] = 0. \quad (\text{A3})$$

For the considered ranges of variables, we see the following. The multiplier of the second derivative and the second summand in the left-hand side of (A3) are both non-negative. Hence, we finally obtain $\partial^2 y / \partial \beta^2 \leq 0$ as claimed.

Appendix B: Exact expressions for the cubic case

In this section, we present auxiliary formulas for the case $t = 3$. According to the standard treatment, the cubic equation of interest is transformed to the reduced form

$$\xi^3 + p\xi + q = 0, \quad \Upsilon_{n-1}^{(3)}(\beta) = \xi - \frac{1}{n^2 - 2n}. \quad (\text{B1})$$

In our case, the coefficients are written as

$$p = -\frac{3(n-1)^2}{(n^2-2n)^2}, \quad q = \frac{3n^2-6n+2}{(n^2-2n)^3} + \frac{1-(n-1)^2\beta}{n^2-2n}. \quad (\text{B2})$$

The real root of the equation (B1) is expressed in line with Cardano's formula (see, e.g., section 1.8-3 of the handbook [81]). Finally, the desired answer is posed by

$$\Upsilon_{n-1}^{(3)}(\beta) = \sqrt[3]{-\frac{q}{2} + \sqrt{Q}} + \sqrt[3]{-\frac{q}{2} - \sqrt{Q}} - \frac{1}{n^2-2n}, \quad Q = \left(\frac{p}{3}\right)^3 + \left(\frac{q}{2}\right)^2. \quad (\text{B3})$$

In the case considered, one should use the principal cube root given that the argument of complex numbers is taken between $-\pi$ and $+\pi$. The cubic equation has three real roots of which at least two are equal, or three different real roots, if Q is zero or negative, respectively [81]. The latter is in agreement with the notes given right after (30). The above expressions are not suitable for $n = 2$. For $n = 2$ and odd t , the equation (A1) reduces to the power $t - 1$. Substituting $n = 2$ and $t = 3$ into (A1) leads to the equation $3y^2 - 3y + 1 = \beta$, whence

$$\Upsilon_1^{(3)}(\beta) = \frac{1}{2} + \sqrt{\frac{4\beta - 1}{12}}. \quad (\text{B4})$$

In a similar manner, one can treat the quartic case. There exist several formulations, mainly due to Ferrari, Descartes and Euler. Explicit easy-to-handle expressions using radicals are presented in [82]. We refrain from reproducing the details here.

-
- [1] Heisenberg W 1927 *Z. Phys.* **43** 172
 - [2] Kennard E H 1927 *Z. Phys.* **44** 326
 - [3] Robertson H P 1929 *Phys. Rev.* **34** 163
 - [4] Busch P, Heinonen T and Lahti P J 2007 *Phys. Rep.* **452** 155
 - [5] Narasimhachar V, Poostindouz A and Gour G 2016 *New J. Phys.* **18** 033019
 - [6] Srinivas M D 2003 *Pramana* **60** 1137
 - [7] Distler J and Paban S 2013 *Phys. Rev. A* **87** 062112
 - [8] Rozpędek F, Kaniewski J, Coles P J and Wehner S 2017 *New J. Phys.* **19** 023038
 - [9] Deutsch D 1983 *Phys. Rev. Lett.* **50** 631
 - [10] Maassen H and Uffink J B M 1988 *Phys. Rev. Lett.* **60** 1103
 - [11] Huang Y 2012 *Phys. Rev. A* **86** 024101
 - [12] Maccone L and Pati A K 2014 *Phys. Rev. Lett.* **113** 260401
 - [13] Wehner S and Winter A 2010 *New J. Phys.* **12** 025009
 - [14] Białynicki-Birula I and Rudnicki Ł 2011 Entropic uncertainty relations in quantum physics *Statistical Complexity* (Berlin: Springer) pp 1–34
 - [15] Coles P J, Berta M, Tomamichel M and Wehner S 2017 *Rev. Mod. Phys.* **89** 015002
 - [16] Hall M J W 2018 *J. Phys. A: Math. Theor.* **51**, 364001
 - [17] Hertz A and Cerf N J 2019 *J. Phys. A: Math. Theor.* **52** 173001
 - [18] Berta M, Christandl M, Colbeck R, Renes J M and Renner R 2010 *Nature Phys.* **6** 659
 - [19] Coles P J and Piani M 2014 *Phys. Rev. A* **89** 022112
 - [20] Berta M, Wehner S and Wilde M M 2016 *New J. Phys.* **18** 073004
 - [21] Coles P J, Colbeck R, Yu L and Żwolak M 2012 *Phys. Rev. Lett.* **108** 210405
 - [22] Friedland S, Gheorghiu V and Gour G 2013 *Phys. Rev. Lett.* **111** 230401
 - [23] Puchała Z, Rudnicki Ł and Życzkowski K 2013 *J. Phys. A: Math. Theor.* **46** 272002
 - [24] Rudnicki Ł, Puchała Z and Życzkowski K 2014 *Phys. Rev. A* **89** 052115
 - [25] Rastegin A E and Życzkowski K 2016 *J. Phys. A: Math. Theor.* **49** 355301
 - [26] Puchała Z, Rudnicki Ł, Krawiec A and Życzkowski K 2018 *J. Phys. A: Math. Theor.* **51** 175306
 - [27] Zozor S, Bosyk G M and Portesi M 2013 *J. Phys. A: Math. Theor.* **46** 465301
 - [28] Zozor S, Bosyk G M and Portesi M 2014 *J. Phys. A: Math. Theor.* **47** 495302
 - [29] Baek K, Farrow T and Son W 2014 *Phys. Rev. A* **89** 032108
 - [30] Zhang J, Zhang Y and Yu C-S 2015 *Quantum Inf. Process.* **14** 2239
 - [31] Rastegin A E 2016 *Ann. Phys. (Berlin)* **528** 835
 - [32] Rastegin A E 2018 *Entropy* **20** 354
 - [33] Durt T, Englert B-G, Bengtsson I and Życzkowski K 2010 *Int. J. Quantum Inf.* **8** 535
 - [34] Renes J, Blume-Kohout R, Scott A and Caves C 2004 *J. Math. Phys.* **45** 2171
 - [35] Scott A J and Grassl M 2010 *J. Math. Phys.* **51** 042203
 - [36] Scott A J 2017 SICs: Extending the list of solutions arXiv:1703.03993 [quant-ph]
 - [37] Appleby M, Bengtsson I, Flammia S and Goyeneche D 2019 *J. Phys. A: Math. Theor.* **52** 295301
 - [38] Appleby D M 2005 *J. Math. Phys.* **46** 052107
 - [39] Fuchs C A, Hoang M C and Stacey B C 2017 *Axioms* **6** 21
 - [40] Appleby M, Flammia S, McConnell G and Yard J 2017 *Found. Phys.* **47** 1042
 - [41] Appleby M and Bengtsson I 2019 *J. Math. Phys.* **60** 062203
 - [42] Delsarte P, Goethals J and Seidel J 1977 *Geom. Dedicata* **6** 363
 - [43] Scott A J 2006 *J. Phys. A: Math. Gen.* **39** 13507
 - [44] Ambainis A and Emerson J 2007 Quantum t -designs: t -wise independence in the quantum world arXiv:quant-ph/0701126
 - [45] Hoggart S G 1982 *Eur. J. Combin.* **3** 233
 - [46] Scott A J 2008 *J. Phys. A: Math. Theor.* **41** 055308

- [47] Roy A and Scott A J 2009 *Des. Codes Cryptogr.* **53** 13
- [48] Dankert C, Cleve R, Emerson J and Livine E 2009 *Phys. Rev. A* **80** 012304
- [49] Bae J, Hiesmayr B C and McNulty D 2019 *New J. Phys.* **21** 013012
- [50] Ketterer A, Wyderka N and Gühne O 2019 *Phys. Rev. Lett.* **122** 120505
- [51] Czartowski J, Goyeneche D, Grassl M and Życzkowski K 2019 *Phys. Rev. Lett.* **124** 090503
- [52] Ketterer A and Gühne O 2020 *Phys. Rev. Research* **2** 023130
- [53] Rastegin A E 2013 *Eur. Phys. J. D* **67** 269
- [54] Conway J H and Sloane N J A 1998 *Sphere Packing, Lattices and Groups* (New York: Springer-Verlag)
- [55] Bengtsson I and Życzkowski K 2017 *Geometry of Quantum States: An Introduction to Quantum Entanglement* (Cambridge: Cambridge University Press)
- [56] Seymour P D and Zaslavsky T 1984 *Adv. Math.* **52** 213
- [57] Hardin R H and Sloane N J A 1996 *Discrete Comput. Geom.* **15** 429
- [58] Gross D, Audenaert K and Eisert J 2007 *J. Math. Phys.* **48** 052104
- [59] Rényi A 1961 On measures of entropy and information *Proceedings of the 4th Berkeley Symposium on Mathematical Statistics and Probability* (Berkeley, CA: University of California Press) pp 547–61
- [60] Kamimura R 1998 *Algorithmica* **22** 173
- [61] Jizba P and Arimitsu T 2004 *Ann. Phys.* **312** 17
- [62] Rastegin A E 2012 *Kybernetika* **48** 242
- [63] Rastegin A E 2015 *RAIRO–Theor. Inf. Appl.* **49** 67
- [64] Rastegin A E 2019 *Quantum Inf. Process.* **18** 276
- [65] Rastegin A E 2016 *Graphs Combin.* **32** 2625
- [66] Mandayam P, Wehner S and Balachandran N 2010 *J. Math. Phys.* **51** 082201
- [67] Ng H Y N, Berta M and Wehner S 2012 *Phys. Rev. A* **86** 042315
- [68] Vermersch B, Elben A, Dalmonte M, Cirac J I and Zoller P 2018 *Phys. Rev. A* **97** 023604
- [69] Landau H J and Pollak H O 1961 *Bell Syst. Tech. J.* **40** 65
- [70] Miyadera T and Imai H 2007 *Phys. Rev. A* **76** 062108
- [71] Bosyk G M, Zozor S, Portesi M, Osán T M and Lamberti P W 2014 *Phys. Rev. A* **90** 052114
- [72] de Vicente J I and Sánchez-Ruiz J 2005 *Phys. Rev. A* **71** 052325
- [73] Rastegin A E 2015 *Open Syst. Inf. Dyn.* **22** 1550005
- [74] Wiseman H M, Jones S J and Doherty A C 2007 *Phys. Rev. Lett.* **98** 140402
- [75] Uola R, Costa A C S, Nguyen H C and Gühne O 2020 *Rev. Mod. Phys.* **92** 15001
- [76] Kriváchy T, Fröwis F and Brunner N 2018 *Phys. Rev. A* **98** 062111
- [77] Teixeira A, Matos A and Antunes L 2012 *IEEE Trans. Inf. Theory* **58** 4273
- [78] Fehr S and Berens S 2014 *IEEE Trans. Inf. Theory* **60** 6801
- [79] Arimoto S 1977 Information measures and capacity of order α for discrete memoryless channels *Topics in Information Theory (Colloquia Mathematica Societatis János Bolyai Vol 16)* (Amsterdam: North-Holland) pp 41–52
- [80] Iwamoto M and Shikata J 2014 Secret sharing schemes based on min-entropies *2014 IEEE Int. Symp. on Information Theory* pp 401–05
- [81] Korn G A and Korn T M 2000 *Mathematical Handbook for Scientists and Engineers* (New York: Dover)
- [82] Yacoub M D and Fraidenraich G 2012 *Math. Gaz.* **96** 271